International Journal of Pharmaceutical Research and Applications
Volume 8, Issue 3 May-June 2023, pp: 3434-3442 www.ijprajournal.com ISSN: 2249-7781

Enhanced Acetone Sensing Performance of Ag-Doped ZnO Thin Films for Non-Invasive Diabetes Detection

C. Rajan[1,*], N.Pasupathy[1], R. Murugesan[2], J.Gobinath[3]

1.Department of Electronics, Research and Development Centre, Erode Arts and Science College (Autonomous), Erode-638009, India

2.Department of Electronics, Research and Development Centre, Erode Arts and Science College (Autonomous), Erode-638009, India

3.Department of Electronics, Research and Development Centre, Erode Arts and Science College (Autonomous), Erode-638009, India

Submitted: 20-06-2023 Accepted: 29-06-2023

ABSTRACT: This paper presents a comprehensive investigation of the enhanced acetone sensing properties of silver-doped zinc oxide (Ag-ZnO) thin films prepared using the sol-gel dip coating method for non-invasive diabetes detection through breath analysis. The structural, morphological, optical, and gas sensing characteristics of the thin films were systematically studied using various characterization techniques. X-ray diffraction (XRD) analysis revealed the formation of a highly crystalline wurtzite structure for both undoped and Ag-doped ZnO thin films. The presence of silver doping induced a shift in the XRD peaks, indicating the successful incorporation of silver into the ZnO lattice. Scanning electron microscopy (SEM) images exhibited a change in the surface morphology of the thin films with increasing silver doping concentration. The grain size was observed to increase, and the surface roughness was reduced, resulting in smoother film surfaces. UV-visible spectrophotometry measurements demonstrated that Ag-doped ZnO thin films exhibited higher optical transparency compared to undoped films. Additionally, a decrease in the optical bandgap was observed with increasing silver concentration, indicating a modification in the band structure of the films. The gas sensing properties of the thin films were evaluated using an acetone sensing test. The Ag-doped ZnO thin films exhibited enhanced acetone sensing response compared to undoped films. The investigation revealed that the optimal doping concentration of 3 at.% Ag resulted in the highest sensitivity and response of the thin film towards acetone vapour, making it well-suited for diabetes detection.

I. INTRODUCTION:

Diabetes mellitus is a chronic metabolic disorder affecting millions of individuals worldwide. Early detection and monitoring of diabetes are crucial for effective management and prevention of complications. In recent years, there has been growing interest in non-invasive diabetes detection methods, including breath analysis, which offers a promising approach for the development of portable and convenient diagnostic devices [1]. Acetone, one of the volatile organic compounds (VOCs) present in exhaled breath, has been identified as a potential biomarker for diabetes due to its elevated levels in diabetic patients [2]. The breath acetone concentration can vary between individuals and is influenced by various factors such as diet, metabolism, and overall health. However, studies have reported average breath acetone concentrations in normal individuals and patients with diabetes [3].

Type 1 and type 2 diabetes are two distinct forms of diabetes mellitus, a chronic metabolic disorder characterised by elevated blood glucose levels [4]. While they share the same name, they differ in their underlying causes, age of onset, and management strategies. It is important to note that the management and treatment approaches for type 1 and type 2 diabetes differ significantly due to their distinct underlying mechanisms. While type 1 diabetes requires lifelong insulin therapy, type 2 diabetes often involves a combination of lifestyle changes, oral medications, and, in some cases, insulin or other injectable therapies [5]. Regular monitoring of blood glucose levels, as well as routine healthcare management, are essential for both types of diabetes to prevent complications and maintain optimal health.

In individuals without diabetes (non-diabetic individuals), the average breath acetone

International Journal of Pharmaceutical Research and Applications
Volume 8, Issue 3 May-June 2023, pp: 3434-3442 www.ijprajournal.com ISSN: 2249-7781

concentration is typically low, ranging from 0.9 to 1.8 parts per million (ppm) [6]. This low concentration is attributed to the normal metabolic processes in the body. On the other hand, patients with diabetes, particularly those with uncontrolled or poorly controlled blood glucose levels, may exhibit higher breath acetone concentrations. The increased concentration of breath acetone in diabetes patients is a result of the body's altered metabolic state, specifically the increased production of ketone bodies due to insulin deficiency or insulin resistance. Breath acetone concentrations in patients with diabetes can range from 1.5 to 4 ppm or even higher in cases of diabetic ketoacidosis (DKA), a life-threatening complication characterised by extremely high levels of ketones[7].

In this context, this paper presents a comprehensive investigation of the enhanced acetone sensing properties of silver-doped zinc oxide (Ag-ZnO) thin films. The sol-gel dip coating method was employed for the preparation of these thin films, providing a versatile and cost-effective approach [8]. The study focused on examining the structural, morphological, optical, and gas sensing characteristics of the Ag-ZnO thin films, aiming to optimise their performance for non-invasive diabetes detection through breath analysis.

Zinc oxide (ZnO) has emerged as a promising material for gas sensing applications due to its unique properties, including high sensitivity, low cost, and environmental stability. In particular, ZnO has shown great potential in detecting acetone, a volatile organic compound (VOC) found in human breath that holds significance in non-invasive diabetes detection. ZnO is a direct-bandgap oxide semiconductor renowned for its unique optical and electrical characteristics, rendering it a versatile material applicable in various domains such as UV light-emitting devices [9], UV photodetectors [10], solar cells [11], thin film transistors [12], gas sensors [13], and photocatalysts [14, 15]. To enhance the optical and/or electrical properties of ZnO thin films, they are often doped with other elements [16-19]. Intrinsic ZnO thin films typically exhibit n-type conductivity due to inherent point defects like oxygen vacancies and zinc interstitials. Consequently, achieving stable P-type ZnO materials through doping has become a significant research focus. Theoretical studies suggest that in oxygen-rich environments, Ag serves as a promising candidate for doping to attain P-type ZnO [20]. Consequently, numerous studies have been conducted to investigate the impact of Ag doping on the electrical and optical properties of ZnO [21-27]. Currently, there are limited reports on the influence of annealing time on the physical properties of Ag-doped ZnO thin films. However, the annealing process plays a crucial role in oxide thin films synthesised using wet chemical methods, particularly the sol-gel approach. Thus, this study aims to fabricate Ag-doped ZnO thin films through a facile sol-gel method and explore the effects of annealing time on their physical properties.

In this study, the sol-gel dip coating method was employed for the preparation of zinc oxide (ZnO) thin films due to the following advantages and considerations: Cost-effectiveness,uniform film formation, tailored film properties, versatility in substrate compatibility, compatibility with additive doping, scalability and reproducibility,etc.

The structural analysis of the thin films was performed using X-ray diffraction (XRD) analysis, revealing the formation of a highly crystalline wurtzite structure in both undoped and Ag-doped ZnO films. The successful incorporation of silver into the ZnO lattice was confirmed by the observed shift in XRD peaks. Scanning electron microscopy (SEM) images exhibited changes in the surface morphology of the films with increasing silver doping concentration, including an increase in grain size and smoother film surfaces. Furthermore, UV-visible spectrophotometry measurements demonstrated higher optical transparency in the Ag-doped ZnO films compared to undoped films. The observed decrease in the optical bandgap with increasing silver concentration indicated a modification in the band structure of the films, which could enhance their gas sensing properties.

To evaluate the gas sensing capabilities, an acetone sensing test was conducted on the thin films. The Ag-doped ZnO films exhibited an enhanced response to acetone vapour compared to undoped films, suggesting their potential for selective detection of acetone, a key biomarker for diabetes. The investigation further identified the optimal doping concentration of 3 at.% Ag, which resulted in the highest sensitivity and response towards acetone vapour.

II. MATERIALS & METHODS

To prepare a 0.2 M zinc acetate dihydrate ($Zn(C_3COO)_2{\cdot}2H2O$) solution, 0.746 g of the compound was dissolved in 20 ml of ethanol and stirred until completely dissolved. Similarly, a 0.02

International Journal of Pharmaceutical Research and Applications
Volume 8, Issue 3 May-June 2023, pp: 3434-3442 www.ijprajournal.com ISSN: 2249-7781

M solution of Silver nitrate ($AgNO_3$) was prepared for the production of Ag-doped ZnO thin films. This was achieved by dissolving 0.026 g of Silver nitrate in 20 ml of ethanol and stirring until complete dissolution. To adjust the pH of the ZnO solution to 7, diethanolamine was added drop by drop while continuously stirring the solution. The necessary concentration of silver for Ag-doped ZnO thin films was achieved by combining the appropriate volume of the silver nitrate solution with the ZnO solution. For example, to create 3 at % Ag-doped ZnO, 17 ml of the ZnO solution was mixed with 3 ml of the silver nitrate solution. The resulting mixture was stirred regularly using a magnetic stirrer for an additional two hours to ensure proper mixing. The solution was aged for 24 hours.

Glass substrates were subjected to a series of 10-minute sonications in acetone, ethanol, and deionized water. Afterward, the substrates were dried using nitrogen gas. These clean and dry substrates were then vertically immersed into the solution and withdrawn at a speed of 5 mm/s using an automatic dip coating machine. The coated substrates underwent a drying process at a temperature of 100 °C for 10 minutes to allow the solvent to evaporate. Subsequently, the coated substrates were annealed in air at 500 °C for 2 hours, resulting in the formation of thin films consisting of ZnO and Ag-doped ZnO.

III. RESULTS & DISCUSSION

XRD ANALYSIS:

In order to analyse the structural characteristics of the films, an X-ray diffractometer equipped with a high-resolution detector and a Cu K radiation source was employed for the XRD investigation. The diffraction patterns were recorded with a step size of 0.02° within the 2θ range of 20° to 80°. The study included four distinct samples of ZnO with varying levels of silver doping: pure ZnO, ZnO doped with 1 at% Ag, ZnO doped with 3 at% Ag, and ZnO doped with 5 at% Ag. These samples were respectively referred to as Pure ZnO, AgZ-1%, AgZ-3%, and AgZ-5%. Based on the XRD results depicted in Figure 1, it was observed that each sample exhibited a hexagonal wurtzite crystal structure. This was evidenced by the distinct and well-defined diffraction peak corresponding to the (002) crystal plane, occurring at an angle of 2θ = 34.42°. This peak alignment is consistent with the ZnO c-axis orientation.

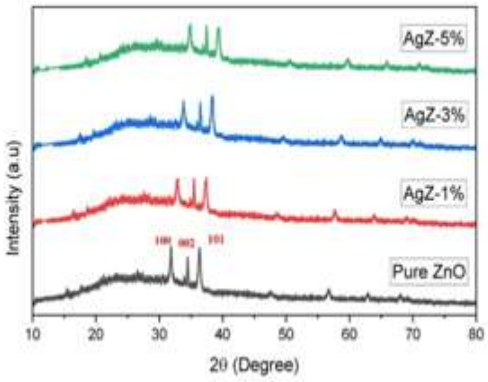

Fig.1.XRD pattern of Pure and Ag doped ZnO films

Table-1 provides a comprehensive overview of the measured diffraction peak angles and their corresponding crystallographic planes for various doping concentrations. The identification of these diffractionpeaks was carried out using the Joint Committee on Powder Diffraction Standards (JCPDS) card no. 36-1451. Upon increasing the concentration of Ag doping, the XRD patterns exhibited a slight shift in the diffraction peaks towards higher angles. This shift signifies the incorporation of A ions into the ZnO lattice. The variation in ionic radii between Zn^{2+} (0.74 Å) and Ag^{3+} (0.53 Å) leads to lattice strain and a marginal reduction in the lattice constant of ZnO. Consequently, the diffraction peaks experience a displacement. The average crystallite size of the thin films was determined using the Scherrer equation, which relies on the full width at half maximum (FWHM) of the (002) peak. For pure ZnO and Ag-doped ZnO, the calculated crystallite sizes ranged from 28.1 to 33.5 nm and 21.3 to 31.1 nm, respectively. The introduction of Ag ions hampers grain growth, thereby causing a decrease in crystallite size with increasing Ag doping concentration.

International Journal of Pharmaceutical Research and Applications
Volume 8, Issue 3 May-June 2023, pp: 3434-3442 www.ijprajournal.com ISSN: 2249-7781

Table 1: Doping concentration, crystallographic planes, and diffraction angles for ZnO and AgZ thin films

Doping Concentration	Crystallographic Planes		
	(100)	(002)	(101)
Pure ZnO	31.82^o	34.42^o	36.31^o
AgZ-1%	32.73^o	35.45^o	37.48^o
AgZ-3%	33.89^o	36.47^o	38.37^o
AgZ-5%	34.91^o	37.41^o	39.47^o

SEM ANALYSIS

Fig.2 illustrates the surface morphology images of the Ag-doped ZnO thin films. All films exhibit flowers like ZnO grains within the plane, with the exception of pureZnO. As the concentration of Ag doping increases, the size of ZnO grains gradually enlarges. This indicates that Ag doping does not significantly affect the crystal growth of ZnO, possibly due to the relatively low Ag doping concentration. Currently, reported findings regarding the impact of Ag doping on ZnO crystal growth are inconsistent. For instance, Liu et al. [28] reported that Ag doping resulted in smaller ZnO grains, while Zhang et al. [29] observed non-uniform grain sizes in Ag-doped ZnO thin films compared to pure ZnO thin films. However, Liu et al. [30] found that Ag doping led to smaller ZnO grains at low Ag doping concentrations, but at higher concentrations, Ag nanoparticles were formed instead. Surprisingly, despite the precipitation of Ag nanoparticles, the crystallinity of ZnO does not diminish. On the contrary, the ZnO grains exhibit growth with an increase in Ag nanoparticles. The observed variations in the effects of Ag doping on ZnO grain growth can be attributed to the different lattice sites occupied by Ag in ZnO, influenced by various film deposition methods and annealing treatments. In our samples, it is evident that Ag doping has minimal influence on ZnO grain growth and does not result in significant nonuniformity in grain size. However, in the case of sample AgZ-5 at %, an increase in surface pores is observed. This increase in pores may be attributed to an elevated presence of gasification substances within the film due to a higher concentration of dopants. The presence of pores is commonly observed in films deposited using the sol-gel method. From the SEM image, particles are estimated to have a diameter of approximately 22 nm, indicating the presence of Ag nanoparticles. Similar findings have been reported by Houng and Huang [31].

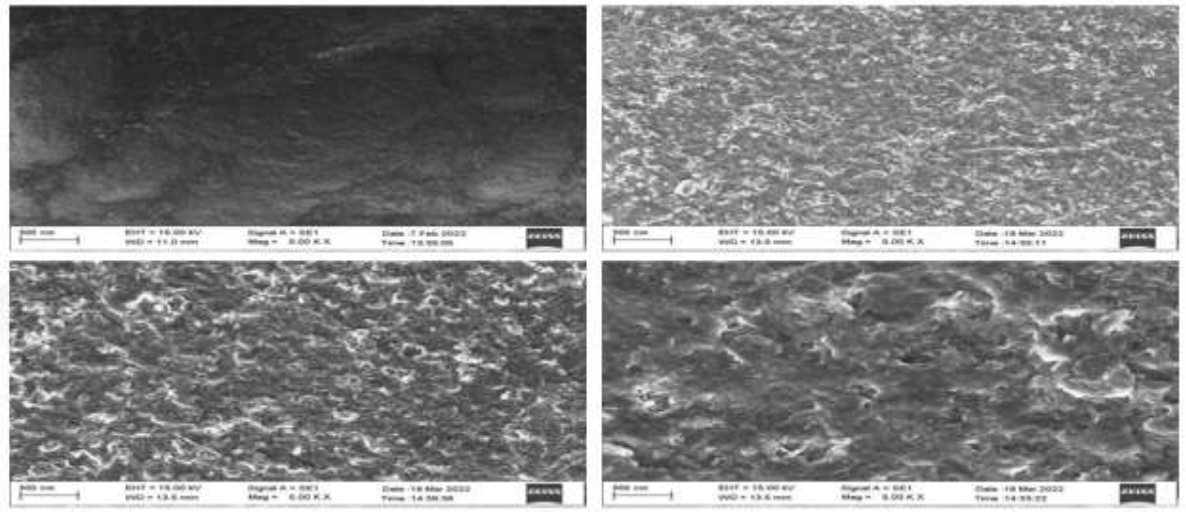

Fig.2. SEM images of (a) Pure ZnO (b) AgZ-1% (c) AgZ-3% (d) AgZ-5

International Journal of Pharmaceutical Research and Applications
Volume 8, Issue 3 May-June 2023, pp: 3434-3442 www.ijprajournal.com ISSN: 2249-7781

UV ABSORBANCE:

UV-Vis spectroscopy was conducted using a UV-Vis spectrophotometer, covering a wavelength range of 200 to 800 nm. The purpose was to analyse the films and determine their band gap energy and absorption behaviour. Both pure ZnO and Ag-doped ZnO thin films exhibited distinct UV absorption edges and transparent regions in the visible spectrum. The absorption edge is attributed to the material's electronic transitions from the valence band to the conduction band. Upon increasing the concentration of Ag dopants, the absorption edge of the films shifted towards longer wavelengths (redshift) [32]. This indicates that the incorporation of Ag ions into the ZnO lattice led to a reduction in the films' band gap energy [33]. The presence of Ag dopants created intermediate energy levels within the bandgap, causing the observed redshift. These optical absorption characteristics and bandgap energies play a crucial role in the sensing applications of the thin films.

In particular, the Ag-doped ZnO thin films are well-suited for acetone sensing due to their ability to provide higher sensitivity within the required wavelength range. This is achieved through the redshift in the absorption edge and the tunability of the bandgap energy achieved by Ag doping. The absorbance graph is shown in Fig.3.

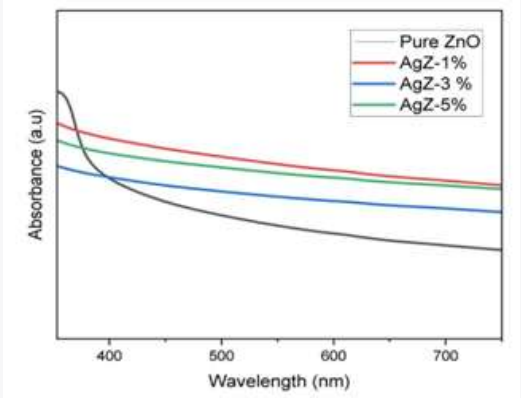

Fig.3: Absorbance Graph

BAND GAP

The determination of the bandgap energy (Eg) for the films was performed using the Tauc plot method. The Tauc plot involves plotting $(\alpha h\upsilon)^2$ against the photon energy ($h\upsilon$), where $h\upsilon$ represents the photon energy and α represents the absorption coefficient. By identifying the intersection point between the linear region of the Tauc plot and the energy axis, the bandgap energy can be determined.

Table-2:Band gap energy for various doping concentration

Doping Concentration	Band gap Energy(eV)
Pure ZnO	3.146
AgZ-1%	3.135
AgZ-3%	3.127
AgZ-5%	3.128

In this study, the bandgap energy of the pure ZnO thin film was calculated to be 3.146 eV. With an increase in the concentration of Ag doping, the bandgap energy decreased. Specifically, for Ag-doped ZnO thin films with various Ag concentrations and bandgap energies are tabulated (Table-2). This decrease in bandgap energy with increasing Ag doping concentration suggests the formation of an alloyed ZnO:Ag material. The band gap of the AgZ-5% sample was found to have a slight increase compared to other samples. As a result, the AgZ-3% sample demonstrated the highest response among all the samples. Fig. 4 displays the band gap graph, depicting the relationship between $(\alpha h\upsilon)^2$ and photon energy ($h\upsilon$).

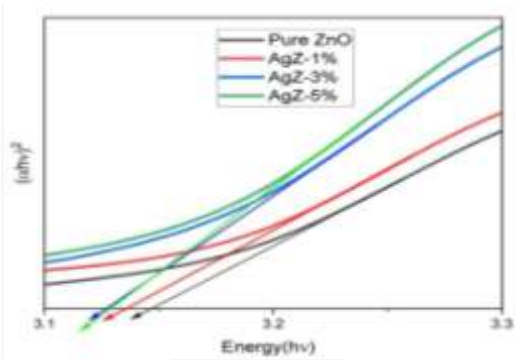

Fig.4: Band gap

SENSING RESPONSE TO ACETONE GAS:

The electrical resistance of both pure and Ag-doped ZnO thin films was measured when exposed to different concentrations of acetone gas (pure, 1 at%, 3 at%, and 5 at%). The results clearly demonstrated the significant impact of Ag doping on the films' ability to sense acetone gas. The sensing performance of the thin films at different acetone gas concentrations is presented in Fig. 5.

International Journal of Pharmaceutical Research and Applications
Volume 8, Issue 3 May-June 2023, pp: 3434-3442 www.ijprajournal.com ISSN: 2249-7781

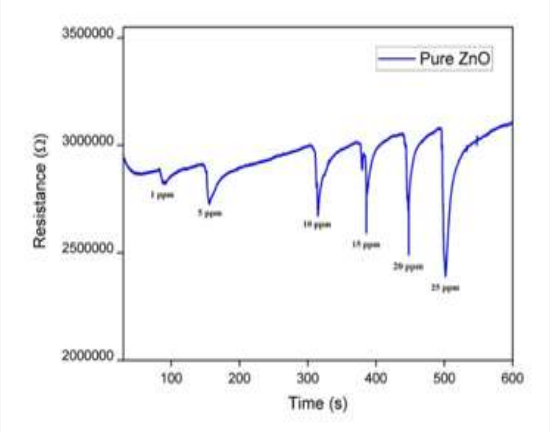

Fig. 5: Response of pure ZnO

Upon exposure to acetone gas, the electrical resistance of the films decreased dramatically, indicating an increase in conductivity due to the interaction between acetone molecules and the film surface. This change in resistance can be attributed to the charge transfer mechanisms and surface reactions that occur when acetone molecules are adsorbed onto the film surface [34].

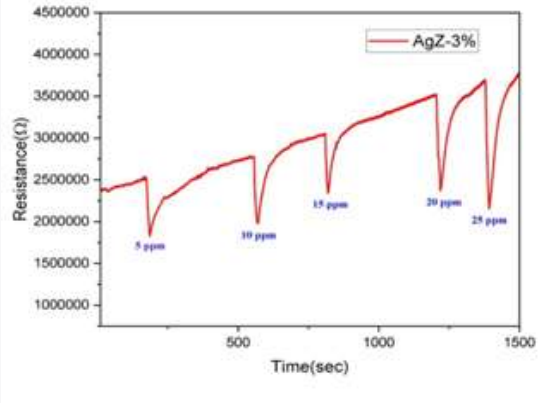

Fig.6: Response of ZnO doped with 3 at% Ag

The 3% Ag-doped ZnO thin film exhibited the highest response among all the samples, showing a significant decrease in resistance compared to both the pure ZnO film and the other Ag-doped films. The incorporation of Ag ions into the ZnO lattice introduces defects and increases the number of adsorption sites for acetone molecules. This enhanced response was evaluated by calculating the percentage change in resistance using the following formula, which allows for the assessment of the sensitivity of the thin films to acetone gas:

$$\text{Response} = [(R_0 - R_{gas}) / R_0] \times 100\%$$

Where, R_{gas} is the film's resistance in the presence of acetone gas and R_0 is the film's initial resistance. Upon exposure to 10 ppm of acetone at room temperature, the 3% Ag-doped ZnO thin film exhibited maximum sensitivity to acetone gas, showing a response of 49%. This indicates the film's high sensitivity and ability to detect low concentrations of acetone gas.

To assess the selectivity of the thin films towards acetone, they were tested against various interfering gases such as ammonia, methanol, ethanol, and isopropanol. The results demonstrated the films' good selectivity for acetone, as they exhibited low sensitivity to the interfering gases. This selectivity is crucial in practical applications where the detection and differentiation of specific target gases are required. The selectivity graph is depicted in Fig. 7.

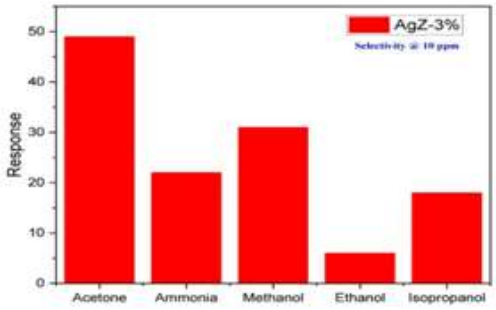

Fig. 7: Selectivity graph

TABLE-2. Analysing acetone detection: new findings versus literature

Material	Temperature (^oC)	Method	Acetone (ppm)	Response time (s)	Recovery time (s)	Reference
ZnO:Ag	RT	Sol-gel	5	9	17	This work
ZnO:Al	500	Hydrothermal	1	147	181	35
ZnO:Al	500	Hydrothermal	0.5	78	113	35

International Journal of Pharmaceutical Research and Applications
Volume 8, Issue 3 May-June 2023, pp: 3434-3442 www.ijprajournal.com ISSN: 2249-7781

ZnO:Al	500	Hydrothermal	0.1	44	70	35
ZnO:Al	450	Hydrothermal	10	3	-	36
ZnO:Al:Pt	450	Magnetron Sputtering	10	2.9	-	37
ZnO:CuO	310	Sol-gel	0.2	7	10	38
ZnO:Au	300	Wet-chemical	0.1	6	24	39
ZnO	RT	Sol-gel	5	12	7	40

The dynamic performance of the thin films was evaluated by analysing their response and recovery times. The response time represents the duration it takes for the resistance to stabilise after exposure to acetone gas, while the recovery time indicates the time it takes for the resistance to return to its initial value once the acetone gas is removed.The 3% Ag-doped ZnO thin film exhibited a fast response time of 9 seconds, indicating its ability to rapidly detect changes in acetone concentration. Additionally, it demonstrated a recovery time of 17 seconds, indicating a quick return to its initial state once the acetone gas was eliminated. Based on these response and recovery durations, the 3% Ag-doped ZnO thin film exhibits promising dynamic performance, making it a potential candidate for real-time acetone gas sensing applications. Table 2 presents a comparison between the acetone detection results obtained in the current investigation and those reported in previous studies.

IV.CONCLUSION:

In conclusion, this research paper provides a comprehensive investigation into the enhanced acetone sensing properties of silver-doped zinc oxide (Ag-ZnO) thin films for non-invasive diabetes detection through breath analysis. The study employed the sol-gel dip coating method to prepare the thin films, and various characterization techniques were utilised to analyse their structural, morphological, optical, and gas sensing characteristics. The X-ray diffraction analysis confirmed the formation of a highly crystalline wurtzite structure in both undoped and Ag-doped ZnO thin films, with the latter showing a shift in the XRD peaks due to successful incorporation of silver into the ZnO lattice. Scanning electron microscopy revealed changes in surface morphology, including increased grain size and reduced surface roughness, resulting in smoother film surfaces with higher optical transparency observed through UV-visible spectrophotometry. The gas sensing properties of the thin films were evaluated specifically for acetone sensing, a biomarker associated with diabetes. The Ag-doped ZnO thin films exhibited enhanced acetone sensing response compared to undoped films, indicating their potential for diabetes detection. The investigation further identified that a doping concentration of 3 at.% Ag resulted in the highest sensitivity with response and recovery time 9sec and 17 sec respectively towards acetone vapour.

Overall, this research contributes valuable insights into the development of improved sensing materials for non-invasive diabetes detection, highlighting the potential of Ag-ZnO thin films prepared via the sol-gel dip coating method as a promising platform for future applications in breath analysis and healthcare diagnostics.

REFERENCE

[1]. Siddiqui S.A., Zhang Y., Lloret J., Song H., Obradovic Z. Pain-Free Blood Glucose Monitoring Using Wearable Sensors: Recent Advancements and Future Prospects. IEEE Rev. Biomed. Eng. 2018;**11**:21–35. doi: 10.1109/RBME.2018.2822301.

[2]. Righettoni M., Tricoli A., Gass S., Schmid A., Amann A., Pratsinis S.E. Breath acetone monitoring by portable Si: WO3 gas sensors. Anal. Chim. Acta. 2012;738:69–75. doi: 10.1016/j.aca.2012.06.002.

[3]. Sun M., Wang Z., Yuan Y., Chen Z., Zhao X. Continuous Monitoring of Breath Acetone, Blood Glucose and Blood Ketone in 20 Type 1 Diabetic Outpatients

International Journal of Pharmaceutical Research and Applications
Volume 8, Issue 3 May-June 2023, pp: 3434-3442 www.ijprajournal.com ISSN: 2249-7781

Over 30 Days. J. Anal. Bioanal. Tech. 2017;8:2155–9872. doi: 10.4172/2155-9872.1000386.

[4]. Tan, S. Y., Wong, J. L. M., Sim, Y. J., Wong, S. S., Elhassan, S. A. M., Tan, S. H., ... &Candasamy, M. (2019). Type 1 and 2 diabetes mellitus: A review on current treatment approach and gene therapy as potential intervention. Diabetes & metabolic syndrome: clinical research & reviews, 13(1), 364-372.

[5]. Igel, L. I., Powell, A. G., Apovian, C. M., & Aronne, L. J. (2012). Advances in medical therapy for weight loss and the weight-centric management of type 2 diabetes mellitus. Current atherosclerosis reports, 14, 60-69.

[6]. Verma, A., Yadav, D., Singh, A., Gupta, M., Thapa, K. B., & Yadav, B. C. (2022). Detection of acetone via exhaling human breath for regular monitoring of diabetes by low-cost sensing device based on perovskite BaSnO3 nanorods. Sensors and Actuators B: Chemical, 361, 131708.

[7]. W. Chuji, A. Mbi, M. Shepherd, A study on breath acetone in diabetic patients using a cavity ringdown breath analyzer: exploring correlations of breath acetone with blood glucose and glycohemoglobin A1C, Sens. J. IEEE 10 (2010) 54–63

[8]. Choi A.H. and Ben-Nissan B. (2014). Advancement of sol- gel technology and nanocoatings in Australia. Journal of the Australian Ceramics Society, 50, 121-136.

[9]. R. Deng, B. Yao, Y. F. Li, Y. Xu, J. C. Li, B. H. Li, Z. Z. Zhang, L. G. Zhang, H. F. Zhao, D. Z. Shen, Ultraviolet electroluminescence from n-ZnO/p-NiO heterojunction light-emitting diode, Journal of Luminescence 134 (2013) 240.

[10]. M. Soylu, F. Yakuphanoglu, Fabrication and characterization of light-sensing device based on transparent ZnO thin film prepared by sol-gel, Optik 127 (2016) 8479.

[11]. A. M. S. Salem, S. M. El-Sheikh, Farid A. Harraz, S. Ebrahim, M. Soliman, H. S. Hafez, I. A. Ibrahim, M. S. A. Abdel-Mottaleb, Inverted polymer solar cell based on MEH-PPV/PC61BM coupled with ZnO nanoparticles as electron transport layer, Applied Surface Science 425 (2017) 156.

[12]. Teresa Oh, Tunnelling condition at high Schottky barrier and ambipolar transfer characteristics in zinc oxide semiconductor thin film transistors, Materials Research Bulletin 77 (2016) 1.

[13]. Z. X. Yu, Y. Z. Ma Y. L. Zhao, J. B. Huang, W. Z. Wang, M. Moliere, H. L. Liao, Effect of precursor solutions on ZnO film via solution precursor plasma spray and corresponding gas sensing performances, Applied Surface Science 412 (2017) 683

[14]. Partha Kumbhakar, Subrata Biswas, Pathik Kumbhakar, Observation of high photocatalytic activity by tuning of defects in chemically synthesised ethylene glycol capped ZnO nanorods, Optik 154 (2018) 303.

[15]. L. Xu, G. Zheng, F. Xian, J. Su, W. Rao, The photocatalytic performance of ZnO/Ag multi-layered films: the effect of ZnO-layer thickness, Optoelectronics and Advanced Materials-Rapid Communications 11 (2017) 381.

[16]. Z. Q. Xu, H. Deng, Y. Li, Q. H. Guo, Y. R. Li, Characteristics of Al-doped c-axis orientation ZnO thin films prepared by the sol–gel method, Materials Research Bulletin 41 (2006) 354.

[17]. Yang Geng, Li Guo, Sai-Sheng Xu, Qing-Qing Sun, Shi-Jin Ding, Hong-Liang Lu, David Wei Zhang, Influence of Al doping on the properties of ZnO thin films grown by atomic layer deposition, The Journal of Physical Chemistry C 115 (2011) 12317.

[18]. A. J. Kulandaisamy, J. R. Reddy, P. Srinivasan, K. J. Babu, G. K. Mani, P. Shankar, J. B. B. Rayappan, Room temperature ammonia sensing properties of ZnO thin films grown by spray pyrolysis: Effect of Mg doping, Journal of Alloys and Compounds 688 (2016) 422.

[19]. N. Rana, S. Chand, A. K. Gathanian, Tailoring the structural and optical properties of ZnO by doping with Cd, Ceramics International 41 (2015) 12032.

[20]. Yanfa Yan, M. M. Al-Jassim, Su-Huai Wei, Doping of ZnO by group-IB elements, Applied Physics Letters 89 (2006) 181912

[21]. Rui Deng, Youming Zou, Honggao Tang, Correlation between electrical, optical properties and Ag2+ centres of ZnO:Ag thin films, Physica B 403 (2008) 2004.

[22]. Eun-Kyung Jeong, In Soo Kim, Dae-Hyun Kim, Se-Young Choi, Effect of deposition and annealing temperature on structural, electrical and optical properties of Ag doped ZnO thin films, Korean Journal of Materials Research, 18 (2008) 84.

[23]. In Soo Kim, Eun-Kyung Jeong, Do Yun Kim, Manoj Kumar, Se-Young Choi, Investigation of p-type behaviour in Ag-doped ZnO thin films by E-beam evaporation, Applied Surface Science 255 (2009) 4011.

[24]. R. Deng, B. Yao, Y. F. Li, T. Yang, B. H. Li, Z. Z. Zhang, C. X. Shan, J. Y. Zhang, D. Z. Shen, Influence of oxygen/argon ratio on structural, electrical and optical properties of Ag-doped ZnO thin films, Journal of Crystal Growth 312 (2010) 1813.

[25]. M. A. Myers, J. H. Lee, Z. Bi, H. Wang, High quality p-type Ag-doped ZnO thin films achieved under elevated growth temperatures, Journal of Physics: Condensed Matter 24 (2012) 145802.

[26]. T. Touam, F. Boudjouan, A. Chelouche, S. Khodja, M. Dehimi, D. Djouadi, J. Solard, A. Fischer, A. Boudrioua, Effect of silver doping on the structural, morphological, optical and electrical properties of sol–gel deposited nanostructured ZnO thin films, Optik 126 (2015) 5548.

[27]. A. Chelouche, D. Djouadi, H. Merzouk, A. Aksas, Influence of Ag doping on structural and optical properties of ZnO thin films synthesised by the sol–gel technique, Applied Physics A 115 (2014) 613

[28]. K. Liu, B. Yang, H. Yan, Z. Fu, M. Wen, Y. Chen, J. Zuo, Appl. Surf. Sci. 255 (2008) 2052

[29]. Y. Zhang, Z. Zhang, B. Lin, Z. Fu, J. Xu, J. Phys. Chem. B 109 (2005) 19200.

[30]. M. Liu, S.W. Qu, W.W. Yu, S.Y. Bao, C.Y. Ma, Q.Y. Zhang, J. He, J.C. Jiang, E.I. Meletis, C.L. Chen, Appl. Phys. Lett. 97 (2010) 231906.

[31]. B. Houng, C.J. Huang, Surf. Coat. Technol. 201 (2006) 3188.

[32]. You, Qinghu, et al. "Blue shift in absorption edge and widening of the band gap of ZnO by Al doping and Al–N co-doping." Journal of Alloys and Compounds 644 (2015): 528-533.

[33]. Khlayboonme, S. Tipawan, and WarawootThowladda. "Impact of Al-doping on structural, electrical, and optical properties of sol-gel dip coated ZnO: Al thin films." Materials Research Express 8.7 (2021): 076402.

[34]. Tian, Ruonan, et al. "Ru-functionalized Ni-doped dual phases of α/γ-Fe2O3 nanosheets for an optimised acetone detection." Journal of Nanostructure in Chemistry (2022): 1-13.

[35]. R. Yoo, Y. Park, H. Jung, H. Rim, S. Cho, H. Lee, W. Lee, Acetone-sensing properties of doped ZnO nanoparticles for breath analyzer applications, J. Alloys Compd. 803 (2019) 135–144.

[36]. R. Yoo, A.T. Güntner, Y. Park, H.J. Rim, H.S. Lee, W. Lee, Sensing of acetone by Al-doped ZnO, Sensor. Actuator. B Chem. 283 (2019) 107–115.

[37]. A. Koo, R. Yoo, S.P. Woo, H.S. Lee, W. Lee, Enhanced acetone-sensing properties of pt-decorated al-doped ZnO nanoparticles, Sensor. Actuator. B Chem. 280 (2019) 109–119.

[38]. Y. Xie, R. Xing, Q. Li, L. Xu, H. Song, Three-dimensional ordered ZnO-CuO inverse opals toward low concentration acetone detection for exhaled breath sensing, Sensor. Actuator. B Chem. 211 (2015) 255–262.

[39]. F. Meng, N. Hou, Z. Jin, B. Sun, W. Li, X. Xiao, C. Wang, M. Li, J. Liu, Sub-ppb detection of acetone using Au-modified flower-like hierarchical ZnO structures, Sensor. Actuator. B Chem. 219 (2015) 209–217.

[40]. K.Muthukrishnan, M. Vanaraja, S. Boomadevi, R.K. Karn, V. Singh, P.K. Singh, K. Pandiyan, Studies on acetone sensing characteristics of ZnO thin film prepared by sol-gel dip coating, J. Alloys Compd. 673 (2016) 138–143.